



A Journal of the Gesellschaft Deutscher Chemiker

Angewandte Chemie

GDCh

International Edition

www.angewandte.org

Accepted Article

Title: Efficient Catalysts for Green Synthesis of Adipic Acid from Biomass

Authors: Ye Wang, Weiping Deng, Longfei Yan, Binju Wang, Qihui Zhang, Haiyan Song, Shanshan Wang, and Qinghong Zhang

This manuscript has been accepted after peer review and appears as an Accepted Article online prior to editing, proofing, and formal publication of the final Version of Record (VoR). This work is currently citable by using the Digital Object Identifier (DOI) given below. The VoR will be published online in Early View as soon as possible and may be different to this Accepted Article as a result of editing. Readers should obtain the VoR from the journal website shown below when it is published to ensure accuracy of information. The authors are responsible for the content of this Accepted Article.

To be cited as: *Angew. Chem. Int. Ed.* 10.1002/anie.202013843

Link to VoR: <https://doi.org/10.1002/anie.202013843>

Efficient Catalysts for Green Synthesis of Adipic Acid from Biomass

Weiping Deng[†], Longfei Yan[†], Binju Wang[†], Qihui Zhang, Haiyan Song, Shanshan Wang, Qinghong Zhang^{*}, and Ye Wang^{*}

[*] Dr. W. Deng, L. Yan, Prof. Dr. B. Wang, Q. Zhang, H. Song, S. Wang, Prof. Dr. Q. Zhang, Prof. Dr. Y. Wang
State Key Laboratory of Physical Chemistry of Solid Surfaces, Collaborative Innovation Center of Chemistry for Energy Materials, National Engineering Laboratory for Green Chemical Productions of Alcohols, Ethers and Esters, College of Chemistry and Chemical Engineering, Xiamen University
Xiamen 361005 (China)
E-mail: zhangqh@xmu.edu.cn
wangye@xmu.edu.cn

[*] These authors contributed equally to this work.

Supporting information for this article is given via a link at the end of the document.

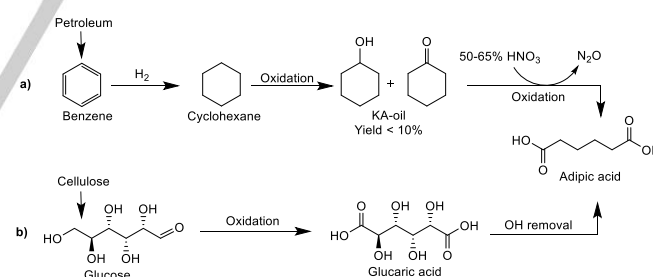
Abstract: Green synthesis of adipic acid from renewable biomass is a very attractive goal of sustainable chemistry. Herein, we report efficient catalysts for a two-step transformation of cellulose-derived glucose into adipic acid via glucaric acid. Carbon nanotube-supported platinum nanoparticles are found to work efficiently for the oxidation of glucose to glucaric acid. An activated carbon-supported bifunctional catalyst composed of rhenium oxide and palladium is discovered to be powerful for the removal of four hydroxyl groups in glucaric acid, affording adipic acid with a 99% yield. Rhenium oxide functions for the deoxygenation but is less efficient for four hydroxyl-group removal. The co-presence of palladium not only catalyzes the hydrogenation of olefin intermediates but also synergistically facilitates the deoxygenation. This work presents a green route for adipic acid synthesis, and offers a bifunctional-catalysis strategy for efficient deoxygenation.

Introduction

Adipic acid is a key monomer for synthesis of important polymers such as nylon-66 and is one of the most important synthetic intermediates in the chemical industry.^[1] Currently, adipic acid is primarily produced by a multi-step process, including the hydrogenation of petroleum-derived benzene to cyclohexane, the subsequent oxidation of cyclohexane into a mixture of cyclohexanone and cyclohexanol (KA oil), and the further oxidation of KA oil to adipic acid by nitric acid (Scheme 1a).^[2] This process not only suffers from high energy-consumption but also has problems of emission of N₂O, a greenhouse and ozone-depletion gas, and low efficiency due to the low single-pass yield (<10%) of KA oil in cyclohexane oxidation.^[2] The development of novel processes for green synthesis of adipic acid becomes urgent because of the increasing need for building green and sustainable chemical society.^[1]

On the other hand, the catalytic valorization of renewable biomass into high-value chemicals has attracted much attention in recent years. As the major component of lignocellulosic biomass, the largest renewable carbon resource on the earth, cellulose, which consists of glucose units connected by β-1,4-glycosidic linkage, is an ideal feedstock for sustainable production of organic oxygenated compounds.^[3] In particular,

cellulose holds the potential for the synthesis of adipic acid because of the six-carbon skeleton of glucose monomer. In addition, sugars including glucose that can be derived from other biomass resources would also play important roles in the sustainable production of chemicals.^[4] A few studies have been devoted to the synthesis of adipic acid or adipate esters through catalytic transformations of biomass-derived C₆ dicarboxylic acids such as 2,5-furandicarboxylic acid (FDCA)^[5] and mucic acid^[6]. However, these C₆ dicarboxylic acids are not easily available, and multiple chemical-reaction^[3a,3e] or biological-fermentation^[6c,6d] processes are required. The synthesis of adipic acid from easily available C₆ sugars, in particular glucose, with one or two steps is a fascinating route, but so far only very limited success has been achieved.^[7]



Scheme 1. Two routes for synthesis of adipic acid. a) The conventional industrial route. b) The biomass-based route.

We focus on developing efficient catalysts for a two-step chemo-catalytic route for the conversion of glucose to adipic acid via glucaric acid (Scheme 1b). In the first step, both the aldehyde and terminal hydroxyl group are oxidized to carboxylic groups. Although many studies have been devoted to the selective oxidation of glucose,^[8] gluconic acid, i.e., the product with only the aldehyde group being oxidized, is the major product in most cases and only limited studies have achieved considerable yields of glucaric acid.^[9] The second step, in which the four hydroxyl groups in glucaric acid need to be removed, is more challenging. Successful strategies to remove multiple hydroxyl groups simultaneously are very scarce. A patent disclosed that the addition of HBr or HI could promote the

cleavage of C–OH bonds in glucaric acid in an acid solvent in the presence of a supported noble metal catalyst under H₂.^[10] The use of corrosive halogen and acid solvent, however, would increase the complexity and cost in reactor design and product separation, and would make the process less green. Deoxydehydration (DODH), an emerging strategy to remove two vicinal hydroxyl groups in diols, has recently been developed for the deoxygenation of biomass-derived alcohols.^[11] Most DODH catalysts, such as rhenium oxide, can only catalyze the conversion of *cis*-diols to olefins. However, in addition to a pair of *cis*-diols, glucaric acid also contains one pair of *trans*-diols, which is difficult to be removed by the DODH catalyst. So far, only a homogeneous rhenium catalyst and a ReO_x/ZrO₂ catalyst have been reported for the deoxygenation of glucaric acid-1,4-lactone with moderate efficiencies, but various promoters or multiple reaction steps are required.^[12] The development of heterogeneous catalysts for one-step conversion of glucaric acid into adipic acid still remains a challenging goal.

Herein, we report a combination of heterogeneous catalysts for the synthesis of adipic acid from glucose via glucaric acid with an overall yield of 81%. Carbon nanotube-supported platinum nanoparticles (Pt/CNT) are found to catalyze the selective oxidation of glucose to glucaric acid. We demonstrate that a bifunctional catalyst composed of rhenium oxide and palladium on activated carbon (Pd–ReO_x/AC) is very efficient for the removal of hydroxyl groups in a variety of biomass-derived carboxylic acids and offers adipic acid with a yield of 99% in the conversion of glucaric acid. The present work not only presents powerful catalysts to accomplish the green synthesis of adipic acid from glucose but also offers an effective bifunctional-catalysis strategy to remove multiple hydroxyl groups for biomass valorization.

Results and Discussion

For the first step, we chose CNT as a support of metal catalysts for selective oxidation of glucose, since CNT is robust in either basic or acidic medium and may promote the oxidation of alcohol/aldehyde groups through the function of its surface carbonyl/phenol groups as redox mediators.^[13] Gluconic acid was the major product and no glucaric acid was formed on CNT alone (Table S1). The loading of metal nanoparticles could promote glucaric acid formation and the Pt/CNT showed the highest selectivity of glucaric acid among the catalysts investigated. The yield of glucaric acid reached 67% over the Pt/CNT catalyst at 333 K and 1 MPa O₂ in aqueous medium.

The mean size of Pt nanoparticles was found to be a key factor for the formation of glucaric acid. Pt/CNT catalysts with mean sizes of Pt nanoparticles in a range of 2.3–6 nm were fabricated by an ethylene glycol (EG) reduction method, in which the mean size of Pt could be tuned by varying the EG/H₂O molar ratio (Figure S1). The catalyst with a larger mean size of Pt (5.7 nm) provided gluconic acid as the major product (Figure 1a). The decrease in the mean size of Pt decreased the yield of gluconic acid and increased that of glucaric acid. The best glucaric acid yield was attained over the catalyst with a mean size of Pt of 2.5 nm. It is noteworthy that the catalyst with small Pt nanoparticles could also catalyze the formation of short-chain acids including glycolic acid, tartronic acid and tartaric acid. The smaller Pt nanoparticles bear larger fractions of coordinatively unsaturated edge and corner atoms, which are known to be

more active toward different types of reactions including the aerobic oxidation of alcohols.^[14] We speculate that the coordinatively unsaturated Pt atoms accelerate the formation of glucaric acid probably by pushing the further oxidation of gluconic acid but simultaneously lead to C–C bond cleavage.

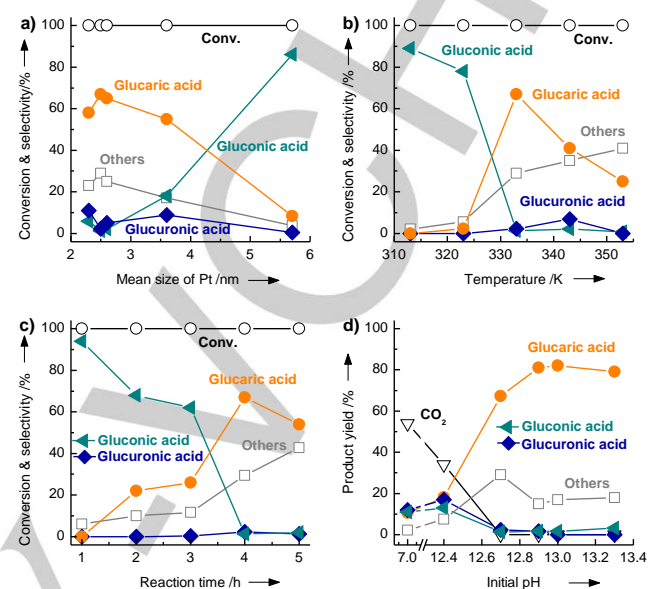
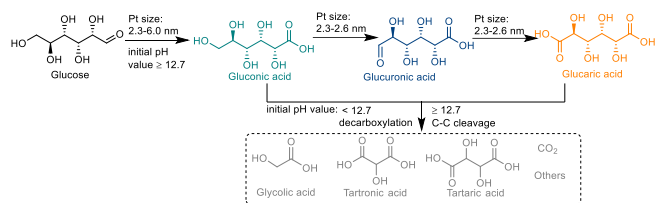


Figure 1. Selective oxidation of glucose over Pt/CNT. a) Effect of mean sizes of Pt particles. b) Effect of reaction temperature. c) Effect of reaction time. d) Effect of initial pH value of reaction medium. Reaction conditions: Pt/CNT (Pt loading 5 wt%), 0.10 g; glucose, 0.50 mmol; H₂O, 20 mL (initial pH = 12.7 except for d); O₂, 1 MPa; temperature, 333 K (except for b); time, 4 h (except for c).

The effects of kinetic parameters on glucose oxidation were investigated for the Pt/CNT catalyst with a mean Pt size of 2.5 nm. The temperature dependence showed that gluconic acid was the major product at 313–323 K (Figure 1b), indicating the preferential occurrence of oxidation of aldehyde group at lower temperatures. As the temperature rose to 333 K, the selectivity of glucaric acid increased at the expense of that of gluconic acid. The time-course analysis demonstrated that gluconic acid was the major product at the initial stage and glucaric acid was formed at longer reaction time at the expense of gluconic acid (Figure 1c). These observations indicate that the formation of glucaric acid proceeds via gluconic acid (Scheme 2). We further propose that glucuronic acid, a product formed by the oxidation of the terminal OH group in gluconic acid, is also an intermediate. The low selectivity of glucuronic acid throughout the reaction probably may arise from the significantly faster oxidation of the aldehyde group as compared to the terminal hydroxyl group in gluconic acid over Pt-based catalysts.^[9a,9b] Thus, once formed, glucuronic acid would be oxidized very quickly to glucaric acid. The control experiment using glucuronic acid as a reactant confirmed that it could be oxidized to glucaric acid more readily than gluconic acid (Table S2). The time-course analysis further showed that the selectivity of short-chain acids increased at longer reaction times (Figure 1c and Table S3). These short-chain acids may be formed in parallel to glucaric acid or by its consecutive oxidation (Scheme 2).

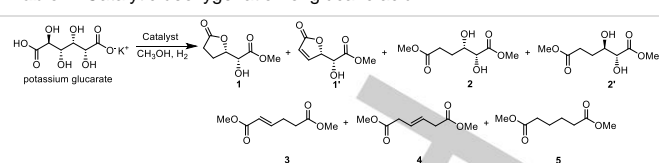


Scheme 2. Proposed reaction mechanism for the oxidation of glucose to glucaric acid over Pt/CNT catalyst.

To suppress the side reactions is the key to boost the efficiency for the formation of glucaric acid. We found that the pH value of the reaction medium played a crucial role in determining the product selectivity (Figure 1d). CO₂ was the major product when the oxidation of glucose was started in the neutral aqueous solution. The pH value of the reactant solution in this case gradually decreased to ~3 due to the formation of acid products. By increasing the initial pH value of the reaction medium with a base (e.g., KOH), the formation of glucaric acid was remarkably enhanced. At an initial pH of 12.9, the yield of glucaric acid, mainly in the form of potassium glucarate, reached 82%. The reaction medium became almost neutral after the reaction. The control experiment using glucaric acid as a reactant confirmed that its degradation was significantly inhibited by increasing the pH of the solution from 6 to 7-9 (Figure S2), indicating the stabilization of glucaric acid in the form of glucarate. We also found that the adsorption of acid products on CNT surfaces became weakened in alkaline aqueous solution (Table S4), indicating that the targeted acid product could be desorbed more facilely from catalyst surfaces under alkaline conditions. These could contribute to the high selectivity of glucaric acid by avoiding the undesirable side reactions.

The second step for the synthesis of adipic acid from glucaric acid by cleaving its four C–OH bonds while keeping the two carboxylic groups intact is more challenging. We first examined a typical DODH catalyst, i.e., ReO₄/AC, for the conversion of potassium glucarate, the product of the first step. A solid acid (Amberlyst-15) was added into the system to help dissolve potassium glucarate by promoting its esterification with methanol, the solvent. In addition to linear methyl glucarate, methyl esters of glucarate lactone were also formed and the molar ratio of linear form to lactone was ~7/3, which did not undergo significant changes with time under reaction conditions in the absence of rhenium catalyst (Figures S3 and S4). This observation suggests the occurrence of esterification equilibrium between linear and lactone forms. The presence of ReO₄/AC catalyzed the deoxygenation reaction of these methyl esters. The major products were those with two hydroxyl groups removed, including product 1, a five-membered ring lactone with one hydroxyl group, product 1', similar to 1 but with an unsaturated alkene in the ring, and products 2 and 2', dimethyl 1,2-dihydroxyhexanedioate, linear esters with two hydroxyl groups in *cis*- or *trans*-form (Table 1). Although the products with four OH groups removed (products 3, 4 and 5) were also formed, the yield of these products was only 27% over the ReO₄/AC catalyst. We speculate that this is because the DODH catalyst is only efficient for the removal of *cis*-diols.^[12] Therefore, new strategies are needed for the removal of all the four OH groups in methyl esters of glucarate or glucarate lactone.

Table 1. Catalytic deoxygenation of glucaric acid.^[a]



Catalyst	Conv. [%]	Product yield [%]				
		1	1'	2&2'	3&4	5
AC	<1	0	0	0	0	0
Pd/AC	7.1	0	0	0	0	0
ReO ₄ /AC	91	21	28	5.8	22	4.8
Pd–ReO ₄ /AC	>99	0	0	0	0	95
Pd–MoO ₄ /AC	25	12	0	0	0	0
Pd–VO ₄ /AC	11	4.3	0	0	0	0
Pd/AC + NH ₄ ReO ₄ ^[b]	94	44	0	0	0	21
Pd/AC + KReO ₄ ^[b]	90	60	0	0	0	18
Pd/AC + HReO ₄ ^[b]	83	63	0	0	0	13
Pd–ReO ₄ /AC- <i>o</i>	>99	0	0	0	0	90
Pd–ReO ₄ /AC- <i>r</i>	98	44	0	0	0	36

[a] Glucaric acid (in the form of potassium salt), 0.10 mmol (25 mg); catalyst (Re, Mo or V loading, 5 wt%; Pd loading, 0.5 wt%), 20 mg; Amberlyst-15, 40 mg; CH₃OH, 5 mL; H₂, 2.0 MPa; 383 K, 24 h. [b] Re accounts for 5 wt% in the mixed catalyst.

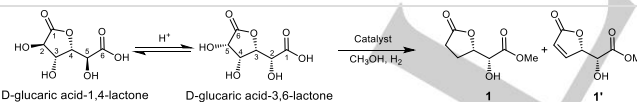
We discovered that the incorporation of a small amount of Pd, which was expected to catalyze the hydrogenation of C=C bond in products 1', 3 and 4, into ReO₄/AC not only saturated the C=C bond but also markedly improved the ability to remove the four OH groups (Table 1). The yield of adipic acid (in the form of methyl ester, product 5) reached 95% over the bifunctional Pd–ReO₄/AC catalyst with Pd and Re loadings of 0.5 wt% and 5 wt%, respectively. Moreover, the Pd–ReO₄/AC catalyst could be recycled at least for 25 times at a reaction time of 6 h and for 10 times at a reaction time of 24 h, and no significant catalyst deactivation was observed (Figure S5). The ReO₄/AC catalysts incorporated with other noble or transition metals such as Pt, Rh, Ir, Cu, Co and Ni were examined for the conversion of potassium glucarate, and the noble metal (Pt, Rh or Ir)-incorporated ReO₄/AC catalyst exhibited >80% yields towards adipic acid (Table S5). The Pd-modified other DODH catalysts including Pd–MoO₄/AC and Pd–VO₄/AC were also investigated, but these catalysts showed much poorer efficiencies for the deoxygenation. It is noteworthy that the Pd–ReO₄/AC catalyst is superior to Pd/AC in combination with homogeneous Re catalysts (NH₄ReO₄, KReO₄ and HReO₄) that are widely used for the deoxygenation reactions.^[11a,11b,12a] Furthermore, our Pd–ReO₄/AC catalyst could catalyze the deoxygenation of a variety of biomass-derived acids such as glucarate lactone, mucic acid, tartaric acid, meso-tartaric acid and gluconic acid (sodium gluconate) (Table S6). The present catalyst could even work for the removal of OH groups in *trans*-diols in spite of the decreased efficiency. To the best of our knowledge, this is the

first efficient heterogeneous catalyst that can work for the conversion of glucaric acid to adipic acid without halide additives.

It is clear that significant synergistic effects exist between Pd and ReO_x for the removal of four OH groups. The Pd/AC alone was almost inactive for the conversion of potassium glucarate, whereas the ReO_x/AC alone was less efficient for the removal of four OH groups. For the bifunctional catalysts with a fixed Pd loading of 0.5 wt%, the yield of product **1** was first increased and then decreased upon increasing the Re loading, whereas the yield of methyl adipate (product **5**) was significantly accelerated at higher Re loadings, reaching 99% as the Re loading became 10 wt% (Table S7). For the bifunctional catalysts with a fixed Re loading of 5 wt%, product **1** was also the major product at a lower Pd loading (0.1 wt%) and an increase in Pd loading to 0.5 wt% significantly enhanced the yield of methyl adipate to 95% (Table S8). These results allow us to propose that ReO_x is the major active component for the removal of OH groups, but Pd should also play a role in the deoxygenation in addition to catalyzing the saturation of C=C bond in products **1'**, **3** and **4**.

To elucidate the role of Pd, we performed kinetic studies for the conversion of glucaric acid-1,4-lactone, a soluble form of glucaric acid in methanol. At the initial reaction stage, both the ReO_x/AC and Pd- ReO_x/AC catalysts could catalyze the removal of two vicinal OH groups, offering products **1'** and **1** as the major products, respectively (Figure S6). We evaluated the intrinsic reaction rates for the two catalysts at the initial reaction stage, where the conversion increased linearly with reaction time (Figure S6). The result demonstrates that the Pd- ReO_x/AC catalyst shows significantly higher conversion rates than the ReO_x/AC at all the temperatures investigated (Table 2). It becomes clear that the presence of Pd significantly accelerated the DODH reaction. We further calculated the activation energies for the two catalysts using the reaction rates displayed in Table 2. The activation energies were 39 and 36 kJ mol^{-1} for the ReO_x/AC and Pd- ReO_x/AC catalysts, respectively (Figure S7). Thus, the presence of Pd does not significantly change the activation energy.

Table 2. Intrinsic reaction rates for the conversion of glucaric acid-1,4-lactone.^[a]



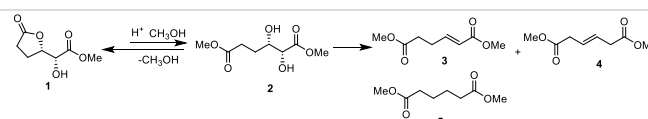
Temperature [K]	Intrinsic rate [$\text{mmol g}^{-1} \text{h}^{-1}$]	
	ReO_x/AC	Pd- ReO_x/AC
323	0	0.51
343	0.44	0.91
363	1.03	1.97
383	1.79	4.22

[a] Glucaric acid-1,4-lactone, 0.10 mmol; Pd- ReO_x/AC (Re loading, 5 wt%; Pd loading, 0.5 wt%), 20 mg; Amberlyst-15, 40 mg; CH_3OH , 5 mL; H_2 , 2.0 MPa. The intrinsic rate was evaluated from Figures S6a and S6c by using the data in the linear region in the early reaction stage.

A comparison of the two catalysts without and with Pd at longer reaction times at 383 K showed that the ReO_x/AC mainly

catalyzed the removal of two vicinal hydroxyl groups from the lactone ring, yielding product **1'** and **1** as the major products, and the further deoxygenation to remove all the hydroxyl groups was difficult even at longer reaction times (Figure S8a). In contrast, the Pd- ReO_x/AC catalyst not only shortened the time required for the formation of product **1** but also significantly accelerated the further deoxygenation of product **1** to methyl adipate (product **5**) at longer reaction times (Figure S8b). We further performed control experiments using **1**, the major reaction intermediate, as the reactant. The result clarified that the Pd/AC was inactive and the sole ReO_x/AC only showed a low efficiency for the conversion of **1** (Table 3). An increase in Re loadings from 5 to 15 wt% in the ReO_x/AC catalyst could increase the conversion of **1**, resulting in an increase in the yield of deoxygenation products (**3**, **4** and **5**). It is of interest that the Pd- ReO_x/AC catalyst with a Re loading of 5 wt% and a Pd loading of 0.5 wt% displayed significantly higher efficiency for the conversion of **1** into methyl adipate (Table 3). This confirms that the co-existence of Pd with ReO_x species accelerates the further deoxygenation of **1**, a key reaction intermediate. It is noteworthy that **1** may undergo reversible reaction to **2** by esterification in methanol. Our calculation reveals that the five-membered ring structure of **1** is energetically more stable than the linear structure of **2** by 9.7 kcal mol^{-1} (Figure S9). Thus, **2** prefers to undergo de-esterification cyclization to **1**. However, if the further deoxygenation of **2** is accelerated, the esterification equilibrium between **1** and **2** would shift to **2**. This can explain why the increase in Re loading in the ReO_x/AC enhances the deoxygenation of **1** (Table 3). As displayed in Table 2, the presence of Pd significantly accelerates the DODH reaction, and thus would facilitate the further DODH of **2** to **5**, contributing to the enhancement in the conversion of **1** to **5** (Table 3). These results provide further evidence that the synergistic effect between Pd and ReO_x works for the removal of vicinal OH groups and the decyclization of ring lactone to accomplish the formation of adipic acid.

Table 3. Catalytic deoxygenation of substrate **1**.^[a]



Catalyst	Conv. [%]	Product yield [%]		
		2	3&4	5
blank	1.5	0.1	0.3	0.8
Pd/AC	1.4	0.3	0	0.9
ReO_x/AC	16	3.6	8.2	4.0
$\text{ReO}_x/\text{AC}^{\text{[b]}}$	38	0.8	27	9.0
$\text{ReO}_x/\text{AC}^{\text{[c]}}$	54	1.0	36	15
Pd- ReO_x/AC	61	0	0	61

[a] Solution of **1** in CH_3OH (15.8 mmol L^{-1}), 5 mL; catalyst (Re loading, 5 wt%; Pd loading, 0.5 wt%), 20 mg; Amberlyst-15, 40 mg; H_2 , 2.0 MPa; 383 K, 4 h.
[b] Re loading is 10 wt%. [c] Re loading is 15 wt%.

To understand the nature behind the synergistic effect between Pd and ReO_x species, we performed characterizations of the ReO_x/AC and $\text{Pd-ReO}_x/\text{AC}$ catalysts. X-ray diffraction (XRD) patterns revealed that ReO_2 and ReO_3 co-existed in both catalysts, and a small diffraction peak assigned to Pd was observed for the $\text{Pd-ReO}_x/\text{AC}$ catalyst (Figure S10). X-ray photoelectron spectroscopy (XPS) measurements indicated that the major surface Re species were similar for both catalysts, including Re^{VI} (33-35%), Re^{V} (57-58%) and a small fraction of Re^{VII} (7.8-8.5%) (Figure S11 and Table S9). No significant changes were observed for the ReO_x/AC and $\text{Pd-ReO}_x/\text{AC}$ catalysts after reactions under conditions of Table 1. High-angle annular dark-field scanning transmission electron microscopy (HAADF-STEM) and energy-dispersive spectroscopy (EDS) elemental mapping results for the ReO_x/AC catalyst showed that large or aggregated ReO_x particles with diameters of 85-300 nm were located on AC (Figure 2a-c). It is of interest that the sizes of ReO_x nanoparticles were significantly reduced to ~20 nm in the presence of Pd (Figure 2d-h). Moreover, a larger fraction of dispersed ReO_x species was found to be in close contact with Pd nanoparticles (diameters of ~20 nm) in the $\text{Pd-ReO}_x/\text{AC}$ catalyst (Figure 2d-h). Hydrogen temperature-programmed reduction (H_2 -TPR) measurements showed that the presence of Pd enhanced the reduction of ReO_x species at lower temperatures (Figure 2i). In situ XRD studies revealed the evolution of crystalline phases in reduction atmosphere with temperatures (Figure S12). For the ReO_x/AC catalyst, ReO_2 and ReO_3 were the sole crystalline phases under H_2 at ≤ 573 K, and the increase in the temperature led to the reduction of ReO_2 and ReO_3 to Re^0 (Figure S12a). On the other hand, a broad diffraction peak at 2θ of 40 - 43° assignable to smaller Re^0 particles began to appear at 473 K for the $\text{Pd-ReO}_x/\text{AC}$ catalyst

under H_2 (Figure S12b). These observations suggest that Pd particles are mainly located nearby ReO_x species on AC, and the presence of Pd not only enhances the dispersion of ReO_x but also facilitates the reduction of the dispersed ReO_x species.

To further identify the possible active rhenium species, we fabricated two reference catalysts, denoted as $\text{Pd-ReO}_x/\text{AC-o}$ and $\text{Pd-ReO}_x/\text{AC-r}$, by oxidative and reductive post-treatment of the $\text{Pd-ReO}_x/\text{AC}$ catalyst in air and H_2 , respectively. Our XPS results revealed that the $\text{Pd-ReO}_x/\text{AC-r}$ catalyst contained a larger fraction of Re^0 (49%) in addition to Re^{V} (33%) and Re^{VI} (18%) on its surfaces, whereas the $\text{Pd-ReO}_x/\text{AC-o}$ catalyst only had surface Re^{VI} (72%) and Re^{VII} (28%) species (Figure S13 and Table S10). The catalytic studies revealed that the $\text{Pd-ReO}_x/\text{AC-r}$ catalyst showed a significantly lower yield of methyl adipate than the $\text{Pd-ReO}_x/\text{AC}$ catalyst (Table 1). On the other hand, the yield of methyl adipate over the $\text{Pd-ReO}_x/\text{AC-o}$ reached 90%, which was much higher than that over the $\text{Pd-ReO}_x/\text{AC-r}$ and only slightly lower than that over the $\text{Pd-ReO}_x/\text{AC}$ catalyst. These observations allow us to speculate that the ReO_x species with a higher Re oxidation state, probably Re^{VI} , might be responsible for the deoxygenation reaction. It is noteworthy that the high-valence Re species such as CH_3ReO_3 and KReO_4 were reported as efficient catalysts for the DODH reactions.^[6,11]

To unravel the catalytic functions of rhenium species in the DODH of diols in glucaric acid, we performed density functional theory (DFT) calculations using a cluster model. An oxo-rhenium cluster, $\text{Re}_{10}\text{O}_{30}$, which was truncated from ReO_3 crystalline structure, was adopted to model the ReO_3 surfaces in DFT calculations (Figure S14). In line with our experiments, the Re atom has an average valence of Re^{VI} in the model. Unlike the bulk phase, one surface rhenium atom (Re_4) is five-coordinated and possesses a vacant coordination site that is available to participate in DODH of diols. 2,3-Dihydroxybutyrolactone was selected as a model substrate. Figure 3 shows the calculated Gibbs energy profiles for the model rhenium cluster-catalyzed DODH of diols. In the initial reactant complex (RC), the proton from O2 maintains a well proton channel to the neighboring $\text{Re}_3=\text{O}$ moiety via the hydroxyl group O1H. Starting from RC, the proton transfer from O1 of 2,3-dihydroxybutyrolactone to the surface $\text{Re}_3=\text{O}$ is quite facile, which involves a Gibbs energy barrier of 4.3 kcal mol⁻¹ for the formation of Re_4-O_2 bond in IC1. To facilitate subsequent dehydration reaction, the O5 atom is dissociated from the central Re_4 atom, with its coordination site being replaced by O2-H (IC1 \rightarrow IC2). The subsequent C-O (both C-O1 and C-O2) cleavage via TS2 leads to the formation of an olefin and oxidized catalyst in IC3, with a Gibbs energy barrier of 25.6 kcal mol⁻¹ relative to IC1. Clearly, two neighboring rhenium sites are cooperatively involved in the dehydration (TS1) and deoxygenation (TS2) reactions. Thus, the true active sites on ReO_3 surfaces can be well represented by a binuclear Re-O-Re site. Such a binuclear rhenium structure of active site on heterogeneous rhenium catalyst functions distinctly different from the mononuclear rhenium active site proposed for the DODH reaction by homogeneous rhenium complexes.^[6b]

Because significant synergistic effects were observed between Pd and ReO_x in the presence of H_2 (Tables 1 and 2), we expect that active H atoms generated from Pd-dissociated H_2 may facilitate the deoxygenation of diols. Accordingly, one H atom has been added into IC1 to remove a water molecule, forming IC2' (Figure 3). Although the energy of IC2' is 6.0 kcal

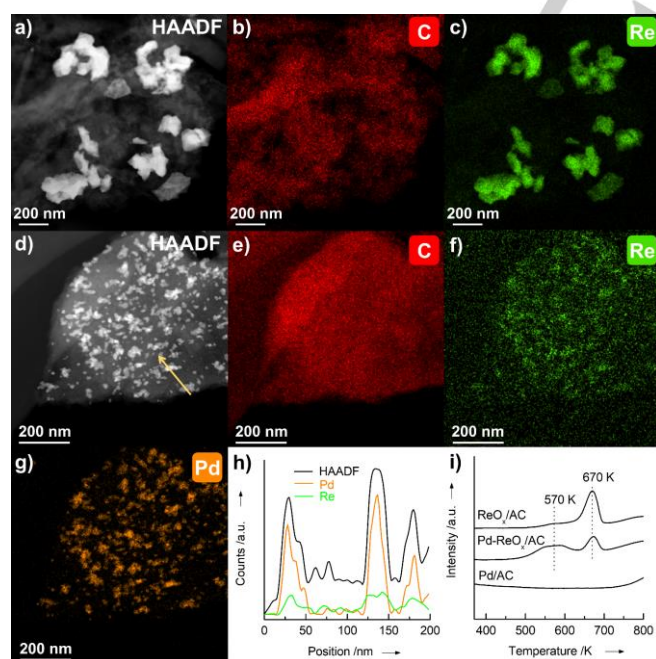


Figure 2. Characterizations of ReO_x/AC and $\text{Pd-ReO}_x/\text{AC}$ catalysts. a) HAADF-STEM image of ReO_x/AC . b) and c), EDS mapping patterns of carbon and rhenium over ReO_x/AC . d) HAADF-STEM image of $\text{Pd-ReO}_x/\text{AC}$. e) EDS mapping patterns of carbon, rhenium and palladium over $\text{Pd-ReO}_x/\text{AC}$. h) Line-scanning elemental distribution for $\text{Pd-ReO}_x/\text{AC}$ along the yellow arrow in d). i) H_2 -TPR profiles.

mol⁻¹ higher than that of IC1, the deoxygenation of IC2' into olefin and the oxidized Re catalyst (PC') becomes quite favorable, which reduces the barrier of deoxygenation by 5.6 kcal mol⁻¹ compared to the route without H-involvement (TS2). Moreover, the subsequent reduction of the oxidized Re species to active site is thermodynamically feasible with H₂ (Figure S15). It is clear that Pd nanoparticles accelerate the reduction of PC' as reflected by the H₂-TPR result. Therefore, we believe that beside C=C hydrogenation, the enhanced dehydration and the regeneration of active sites by Pd-activated H contribute to the significantly higher intrinsic rate of DODH reactions for the Pd-ReO_x/AC catalyst (Figure S6 and Table 2).

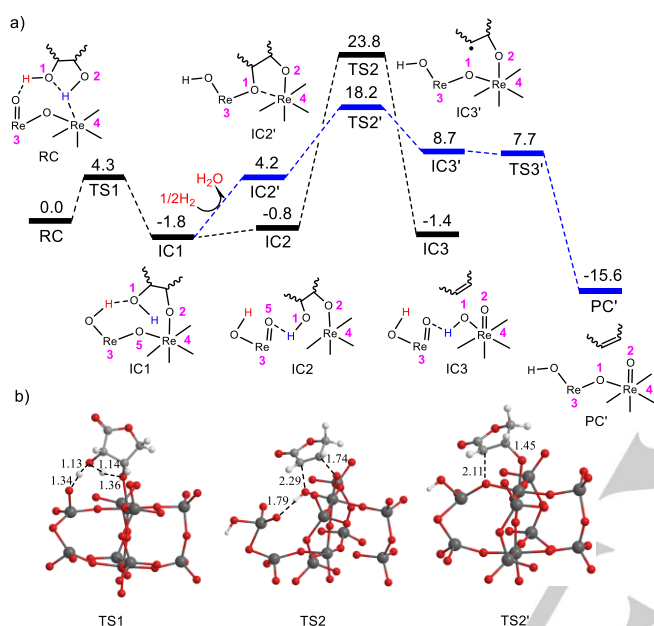
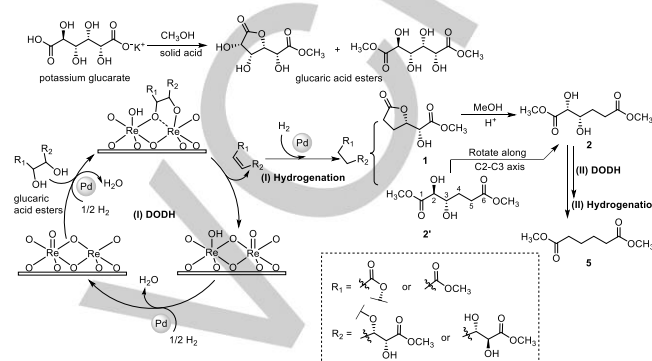


Figure 3. a) DFT-calculated Gibbs energy profile (in kcal mol⁻¹) for the surface ReO₃-catalyzed DODH of diols, shown along with schematic drawings of key intermediates along the reaction pathway. b) Optimized geometries of key transition states involved in the reactions.

In the previous DODH systems catalyzed by oxorhenium complexes, it is generally accepted that the reaction is mediated by the Re^{VII}/Re^V or Re^{VI}/Re^{IV} redox pair and the solvent, typically an alcohol (e.g., 3-pentanol), also functions as a reducing agent.^[6] In our present system, although methanol was used as a solvent, our work revealed that H₂ rather than methanol functioned as the reducing agent. In the absence of H₂, no conversion of potassium gluconate was observed under N₂. The employment of CO instead of H₂ could not induce the reaction (Table S11). Furthermore, the catalytic performance depended on the pressure of H₂; a lower H₂ pressure led to a lower yield of methyl adipate and the yield of methyl adipate reached 95% at a H₂ pressure of ≥ 2 MPa.

Based on the results described above, we propose a possible reaction mechanism for the conversion of gluconic acid catalyzed by the Pd-ReO_x/AC (Scheme 3). In brief, potassium gluconate dissolved in methanol undergoes esterification with methanol, forming both lactone and linear esters in the presence of a solid acid. The ReO_x species, in particular the binuclear Re-O-Re site on ReO₃ surfaces, catalyzes the first DODH reaction of methyl gluconate to corresponding olefins, and the Re-O-Re

site is oxidized at the same time. Pd nanoparticles participate in the DODH reaction by promoting the dehydration of diols via providing active hydrogen from H₂-dissociation. Moreover, Pd also facilitates reduction of the oxidized rhenium site with H₂, accelerating the regeneration of the initial Re-O-Re site. Upon subsequent hydrogenation over the Pd nanoparticle, the saturated intermediates such as **1** and **2'** were transformed further into **2**, which would undergo the second DODH reaction and hydrogenation to yield adipic acid.



Scheme 3. Proposed reaction mechanism for the conversion of gluconic acid (potassium gluconate) to adipic acid (methyl adipate) over Pd-ReO_x/AC catalyst.

We finally performed a tandem conversion of glucose to adipic acid by combining oxidation with the Pt/CNT and deoxygenation with the Pd-ReO_x/AC catalyst, without separation and purification of gluconate, the intermediate product. After glucose oxidation at 333 K and an initial pH of 12.9, the mixed product containing potassium gluconate as well as by-products was collected by freeze-drying of the neutralized reaction solution with the solid catalyst filtered off. The subsequent catalytic deoxygenation of the mixed product in methanol resulted in a methyl adipate yield of 50% based on glucose. The by-products formed in the oxidation of glucose might influence the efficiency of gluconate in the oxidation of glucose is our future research target. We further conducted the conversion of gluconic acid (in the form of potassium gluconate) with higher concentrations. When the concentration of gluconate was increased from 0.60 to 3.0 wt% by increasing its amount from 0.025 to 0.125 g, the yield of methyl adipate was kept at ≥ 95% (Table S12). The increase in the concentration of gluconate to 12 wt% at a Re/gluconate molar ratio of 0.050 resulted in methyl adipate with yield of ≥ 70%. These results demonstrate that the present Pd-ReO_x/AC catalyst is efficient for the conversion of gluconic acid with a higher concentration or at a relatively larger scale to adipic acid.

Conclusion

This work presents a two-step route for green and sustainable synthesis of adipic acid from glucose. Glucose is first oxidized into gluconic acid, which undergoes DODH reaction to form adipic acid after removal of four OH groups. Pt/CNT was found to be an efficient catalyst for the selective oxidation of glucose to gluconic acid, offering a gluconic acid yield of 82%. The catalytic

behaviors of Pt/CNT were dependent on the size of Pt nanoparticles, kinetic parameters (such as temperature and reaction time) and the pH of the reaction solution. Gluconic acid and glucuronic acid were the reaction intermediates, and the oxidation of gluconic acid was a crucial step. We discovered a powerful bifunctional Pd–ReO_x/AC catalyst for the removal of four OH groups in glucaric acid to adipic acid in the form of methyl adipate in methanol and the yield of adipic acid reached 99%. The highly dispersed ReO_x species with rhenium in a high oxidation state (i.e., Re^{VI}) functions for the DODH reaction, while Pd nanoparticles not only catalyze the hydrogenation of C=C bonds in the intermediates but also synergistically facilitate the DODH reaction probably by enhancing the dispersion of ReO_x species and the reduction of ReO_x species. Our DFT calculations suggest that the binuclear Re–O–Re site with one rhenium in five-coordination is responsible for the DODH reaction and the Pd nanoparticles promote both the dehydration of diols and the regeneration of the oxidized ReO_x sites under H₂, providing deep understanding of the synergistic effect between ReO_x and Pd nanoparticles. The Pd–ReO_x/AC catalyst could also be applied to the DODH reaction of several other biomass-derived platform molecules.

Acknowledgements

This work was supported by the National Key R&D program of China (No. 218YFB1501602), the National Natural Science Foundation of China (Nos. 21690082 and 91545203).

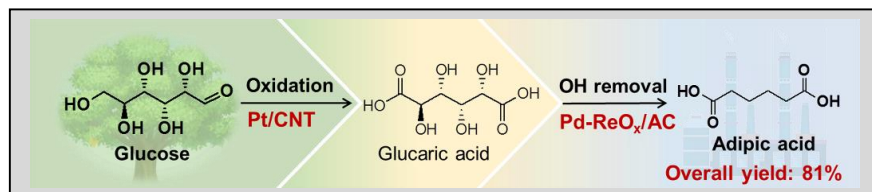
Conflict of interest

The authors declare no conflict of interest.

Keywords: adipic acid • biomass • glucose • heterogeneous catalysis • sustainable chemistry

- [1] a) K. Sato, M. Aoki, R. Noyori, *Science* **1998**, *281*, 1646-1647; b) K. C. Hwang, A. Sagadevan, *Science* **2014**, *346*, 1495-1498; c) J. Yang, J. Liu, H. Neumann, R. Franke, R. Jackstell, M. Beller, *Science* **2019**, *366*, 1514-1517.
- [2] S. Van de Vyver, Y. Román-Leshkov, *Catal. Sci. Technol.* **2013**, *3*, 1465-1479.
- [3] a) S. Van de Vyver, J. Geboer, P. A. Jacobs, B. F. Sels, *ChemCatChem* **2011**, *3*, 82-94; b) A. Wang, T. Zhang, *Acc. Chem. Res.* **2013**, *46*, 1377-1386; c) Z. Zhang, J. Song, B. Han, *Chem. Rev.* **2017**, *117*, 6834-6880; d) S. Li, W. Deng, S. Wang, P. Wang, D. An, Y. Li, Q. Zhang, Y. Wang, *ChemSusChem* **2018**, *11*, 1995-2028; e) A. Shrotri, H. Kobayashi, A. Fukuoka, *Acc. Chem. Res.* **2018**, *51*, 761-768; f) Y. Jing, Y. Guo, Q. Xia, X. Liu, Y. Wang, *Chem* **2019**, *5*, 2520-2546.
- [4] A. Deneyer, T. Ennaert, B. F. Sels, *Curr. Opin. Green Sustain. Chem.* **2018**, *10*, 11-20.
- [5] a) T. Asano, M. Tamura, Y. Nakagawa, K. Tomishige, *ACS Sustainable Chem. Eng.* **2016**, *4*, 6253-6257; b) L. Wei, J. Zhang, W. Deng, S. Xie, Q. Zhang, Y. Wang, *Chem. Commun.* **2019**, *55*, 8013-8016.
- [6] a) M. Shiramizu, F. D. Toste, *Angew. Chem. Int. Ed.* **2013**, *52*, 12905-12909; b) X. Li, D. Wu, T. Lu, G. Yi, H. Su, Y. Zhang, *Angew. Chem. Int. Ed.* **2014**, *53*, 4200-4204; c) D. R. Vardon, M. A. Franden, C. W. Johnson, E. M. Karp, M. T. Guarnieri, J. G. Linger, M. J. Salm, T. J. Strathmann, G. T. Beckham, *Energy Environ. Sci.* **2015**, *8*, 617-628; d) H. Zhang, X. Li, X. Su, E. Ang, Y. Zhang, H. Zhao, *ChemCatChem* **2016**, *8*, 1500-1506.
- [7] K. M. Draths, J. W. Frost, *J. Am. Chem. Soc.* **1994**, *116*, 399-400.
- [8] a) H. Zhang, N. Toshima, *Catal. Sci. Technol.* **2013**, *3*, 268-278; b) M. Besson, P. Gallezot, C. Pinel, *Chem. Rev.* **2014**, *114*, 1827-1870; c) X. Zhang, K. Wilson, A. F. Lee, *Chem. Rev.* **2016**, *116*, 12328-12368; b) Z. Zhang, G. W. Huber, *Chem. Soc. Rev.* **2018**, *47*, 1351-1390.
- [9] a) X. Jin, M. Zhao, J. Shen, W. Yan, L. He, P. S. Thapa, S. Ren, B. Subramaniam, R. V. Chaudhari, *J. Catal.* **2015**, *330*, 323-329; b) X. Jin, M. Zhao, M. Vora, J. Shen, C. Zeng, W. Yan, P. S. Thapa, B. Subramaniam, R. V. Chaudhari, *Ind. Eng. Chem. Res.* **2016**, *55*, 2932-2945; c) J. Lee, B. Saha, D. G. Vlachos, *Green Chem.* **2016**, *18*, 3815-3822; d) E. Derrien, M. Mounquengui-Diallo, N. Perret, P. Marion, C. Pinel, M. Besson, *Ind. Eng. Chem. Res.* **2017**, *56*, 13175-13189.
- [10] T. R. Boussie, E. L. Dias, Z. M. Fresco, V. J. Murphy, J. Shoemaker, R. Archer, H. Jiang, *US8669397B2*, **2014**.
- [11] a) M. Shiramizu, F. D. Toste, *Angew. Chem. Int. Ed.* **2012**, *51*, 8082-8086; b) J. Yi, S. Liu, M. M. Abu-Omar, *ChemSusChem* **2012**, *5*, 1401-1404; c) C. Boucher-Jacobs, K. M. Nicholas, *ChemSusChem* **2013**, *6*, 597-599; d) N. Ota, M. Tamura, Y. Nakagawa, K. Okumura, K. Tomishige, *Angew. Chem. Int. Ed.* **2015**, *54*, 1897-1900; e) J. R. Dethlefsen, P. Fristrup, *ChemSusChem* **2015**, *8*, 767-775; f) S. Raju, M. E. Moret, R. J. M. K. Gebbink, *ACS Catal.* **2015**, *5*, 281-300; g) L. Sandbrink, E. Klindtworth, H. U. Islam, A. M. Beale, R. Palkovits, *ACS Catal.* **2016**, *6*, 677-680; h) M. Tamura, N. Yuasa, J. Cao, Y. Nakagawa, K. Tomishige, *Angew. Chem. Int. Ed.* **2018**, *57*, 8058-8062.
- [12] a) R. T. Larson, A. Samant, J. Chen, W. Lee, M. A. Bohn, D. M. Ohlmann, S. J. Zuend, F. D. Toste, *J. Am. Chem. Soc.* **2017**, *139*, 14001-14004; b) J. Lin, H. Song, X. Shen, B. Wang, S. Xie, W. Deng, D. Wu, Q. Zhang, Y. Wang, *Chem. Commun.* **2019**, *55*, 11017-11020.
- [13] a) X. Wan, C. Zhou, J. Chen, W. Deng, Q. Zhang, Y. Yang, Y. Wang, *ACS Catal.* **2014**, *4*, 2175-2185; b) C. Zhou, W. Deng, X. Wan, Q. Zhang, Y. Yang, Y. Wang, *ChemCatChem* **2015**, *7*, 2853-2863.
- [14] J. Chen, W. Fang, Q. Zhang, W. Deng, Y. Wang, *Chem. Asian J.* **2014**, *9*, 2187-2196.

Entry for the Table of Contents



We present efficient catalysts for green and sustainable synthesis of adipic acid from biomass-derived glucose via glucaric acid. Pt/CNT with smaller Pt nanoparticles (mean size, 2.5 nm) catalyzes the selective oxidation of glucose to glucaric acid. A bifunctional Pd-ReO_x/AC catalyst with significant synergistic effects between Pd and ReO_x offers 99% yield of adipic acid in the conversion of glucaric acid by removal of four hydroxyl groups, and the overall yield of adipic acid reaches 81%.